Mechanical Stability Analysis of the External Unilateral Fixation Device due to the Impact of Axial Pressure

Nedim Pervan
University of Sarajevo, Faculty of Mechanical Engineering, Bosnia and Herzegovina
pervan@mef.unsa.ba (corresponding author)

Elmedin Mesic
University of Sarajevo, Faculty of Mechanical Engineering, Bosnia and Herzegovina
mesic@mef.unsa.ba

Adis Muminovic
University of Sarajevo, Faculty of Mechanical Engineering, Bosnia and Herzegovina
adis.muminovic@mef.unsa.ba

Enis Muratovic
University of Sarajevo, Faculty of Mechanical Engineering, Bosnia and Herzegovina
muratovic@mef.unsa.ba

Muamer Delic
University of Sarajevo, Faculty of Mechanical Engineering, Bosnia and Herzegovina
delic@mef.unsa.ba

Vahidin Hadziabdic
University of Sarajevo, Faculty of Mechanical Engineering, Bosnia and Herzegovina
hadziabdic@mef.unsa.ba

Lejla Redzepagic-Vrazalica
University of Sarajevo, Faculty of Dentistry with Clinics, Bosnia and Herzegovina
lejlaredzepagic@yahoo.com

Received: 27 March 2023 | Accepted: 7 March 2023

 DOI: https://doi.org/10.48084/etasr.5888

ABSTRACT

This study performed a mechanical stability analysis for the impact of axial pressure on an Ultra X external unilateral fixation device applied to a tibia with an open fracture. The real construction of the fixation device was used to create a 3D geometric model using a Finite Element Method (FEM) model, which was made to perform structural analysis in the CATIA V5 (Computer Aided Three-dimensional Interactive Application) CAD/CAE system. Specific stresses and displacements were observed at points of interest using structural analysis. The focus was on the relative displacements of the proximal and distal bone segments in the fracture zone. These displacements were used to calculate the stiffnesses of the bone in the fracture zone and the fixation device itself. The results obtained provide the necessary information regarding the stability of the Ultra X fixation device.

Keywords-external unilateral fixation device; specific stresses; relative displacements, stiffness; stability

I. INTRODUCTION

During the recent years, there has been a considerable improvement in external fixation devices in terms of their construction variants, which have been experimentally investigated to provide information on their characteristics and advantages in terms of stability, stiffness, mechanical properties, and patient comfort during treatment. Using software for 3D modeling and FEM analysis to perform mechanical stability analysis is not a substitution for an experimental examination but is exclusively a tool for data comparison and validation. The experimental investigation of fixation devices is mainly based on biomechanical properties, along with the influence of specific parameters on the stability of the device [1]. The results of these investigations are reflected in certain values, such as von Mises stresses, displacements, angular strains, and fixation device stiffnesses, and most of these studies provide results of the application of the fixation device [2-3].

In recent years, the most popular treatment for tibia fracture is by using intermediary fasteners [4]. In [5], the application of an external fixation device and intermediary fasteners was considered in an open tibia fracture taking into account the treatment time and other possible complications, such as the size, severity, etc. In [6], the stiffness of the fixation device was defined concerning the location of the fracture and the number of fasteners and pins. In [7], an analysis of the stiffness of the Hoofman unilateral and uniplanar fixation device was presented along with its relation to the number of fasteners, trusses, and couplings. The stiffness of the device is determined by the loads that simulate normal walking conditions. In [8], a comparative study was conducted on two external fixation devices: the original Hoffmann and the AO tabular device with four different construction solutions. In [9], the mechanical properties of the external pinless fixation device were experimentally investigated, comparing its results with the AO tabular and Ultra X devices. This study concluded that the AO tabular devices are far superior in comparison with the other two solutions. In [10], the Ilizarov fixation device was investigated experimentally. Furthermore, many studies have analyzed the mechanical stability of structures [11-13]. This study aimed to investigate the mechanical properties of the Ultra X external unilateral fixation device, applied to the open-fracture tibia bone under the impact of axial pressure. The construction parameters taken into account were the stiffness of the device, the values of the maximum von Mises stresses, and the displacements in specific points.

II. DEVELOPMENT OF THE CAD/FEM MODEL

The adjustable fixation device should be light, stiff, easy to implement, etc. Such devices should be part of the first response at accident sites so that basic stabilization could be performed before transporting patients. Figure 1 shows the Howmedic Ultra X external fixation device, which is one of the first modular fixation devices, and was used in the first Gulf War in 1991. The components of the device are mostly made of metals, alloys, and plastics such as polymers and carbon fibers. The Ultra X fixation device has a truss made of austenitic stainless steel X2CrNiMo17-12-2, while couplings and small and large spheres are made of polymeric materials, attributed with smaller strength, Young's modulus, density, specific weight, and great forming properties. The upper and lower parts of the coupling and the fastening head are made of special polyvinyl chloride (PVC), which has high hardness and good mechanical properties. Small and large spheres are made of polybutylene (PB), which has properties similar to PVC because it can be manufactured with any method of thermoforming, and therefore, it gives a lot of creativity during the shape-forming process. Table I shows the mechanical properties of the unilateral Ultra X fixation device [14].

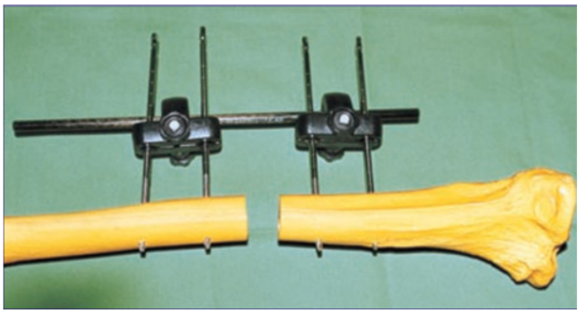

Fig. 1. The Ultra X fixation device.

TABLE I. MECHANICAL PROPERTIES OF THE UNILATERAL ULTRA X FIXATION DEVICE

Component name	**Standard abbreviations (EN)**	**Modulus of elasticity** ***E*** **(GPa)**	**Poisson's coefficient** υ	**Density** ρ **(kg/m3)**	**Yield strength** σv **(MPa)**
Truss	X2CrNiMo17-12-2	230	0.29	8000	620
Sphere	>PB<	2.9	0.4	1290	-
Coupling	>PVC<	3.3	0.38	1380	0.2
Fastener	X5CrNi18-10	193	0.29	7900	205
Half-pin	X2CrNiMo18-14-3	196.4	0.3	8000	800

The CAD/FEM model of the Ultra X device was developed using CATIA V5 software. Device components were defined and modeled in the part design environment and subsequently assembled in the assembly design environment. The General Structural Analysis module was used in the next step of model creation to complete the FEM model and define the material for each component. The material of the bone fragments was assumed to be orthotropic with properties defined according to Table II [15-16]. After the materials were defined, the next step in FEM processing was the discretization of the model and the definition of the finite element type. Linear (TE4) and parabolic (TE10) elements were used for the model. The TE4 elements were used for the spheres, while the rest of the components were discretized with the TE10 elements. After the discretization was complete, it was necessary to define the constraints between the components of the device. The constraints used were the following: fastened connections between half-pins and bone segments, as shown in Figure 2(a), and contact connections between other components, as shown in Figure 2(b). In addition to defining the necessary constraints, it was also mandatory to define supports, as shown in Figure 3.

TABLE II. BONE MODEL MECHANICAL PROPERTIES

Property	Value
Longitudinal modulus of elasticity	22900 MPa
Tangential modulus of elasticity	10500MPa
Normal modulus of elasticity	14200 MPa
Poisson's coefficeint in the XY plane	0.29
Poisson's coefficeint in the XZ plane	0.19
Poisson's coefficeint in the YZ plane	0.31
Shear modulus in the XY plane	6480 MPa
Shear modulus in the XZ plane	6000 MPa
Shear modulus in the YZ plane	3700 MPa
Density	1850 kg/m^3

The last step in creating the FEM model was to define the axial load, which is applied as the surface load on the top surface of the upper bone segment. The upper bone segment is constrained so it can only move in the z-axis direction, i.e. the direction of the applied force. The lower bone segment is supported by a spherical joint (Ball Joint) through a virtual part (Smooth Virtual Part). The spherical joint allows rotation around a predefined point (Handle Node), and all translations are restricted, as shown in Figure 4. The axial load was set to 200 N, according to orthopedic recommendations and [17-18].

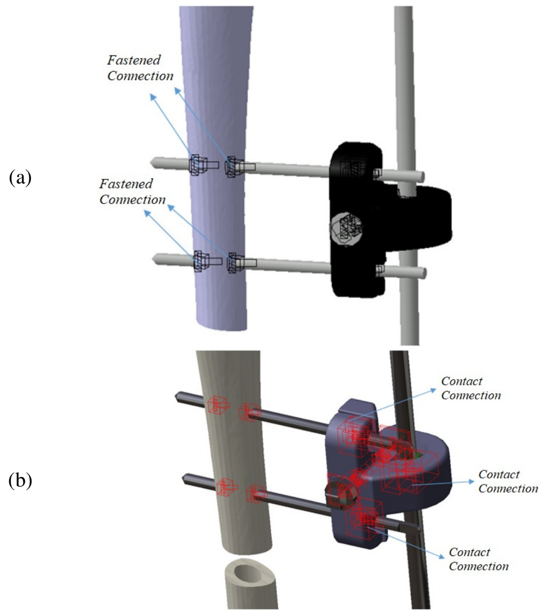

Fig. 2. Defining connection constraints: (a) fastened, (b) contact.

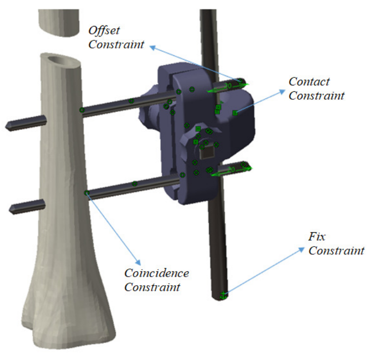

Fig. 3. Fixation device model with constraints and supports.

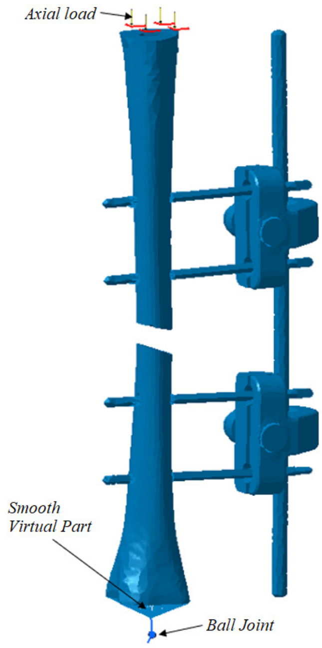

Fig. 4. Fixation device FEM model with the applied load.

III. DETERMINATION OF STRESS, DISPLACEMENT, AND STIFFNESS

During structural analysis, specific points were monitored to obtain values of principal and von Mises stresses generated on the fixation device. The intensity of the equivalent one-axis stress, i.e. von Mises stress, is often used in mechanics defined as [19-20]:

$$\sigma_e = \sigma_{vm} = \sqrt{3J_2} = \sqrt{\frac{1}{2}[(\sigma_1 - \sigma_2)^2 + (\sigma_2 - \sigma_3)^2 + (\sigma_3 - \sigma_1)^2]} \quad (1)$$

Apart from stresses, displacement values at the same points were monitored so the stiffness of the device can be defined as the ratio of the load and displacements. The device stiffness under the impact of axial load can be defined as [19, 21]:

$$C_p = \frac{F_p}{\delta_p} \quad (2)$$

where F_p is the axial force (N), and δ_p is the axial displacement of the bone segments at the fracture zone (mm). The fixation device stiffness is an important parameter, but it doesn't give direct information about displacements at the fracture zone, so the fracture stiffness needs to be defined. This was achieved by determining displacements in the x, y, and z directions of the pair of adjacents points on the planes of the proximal and distal bone segments at the fracture zone. For these points, the resultant vector of relative displacement R_{max} has the highest value. Accordingly, the total fracture stiffness is defined as the ratio of the load and the resultant relative displacement of the observed pair of points [22-23]:

$$C_{pp} = \frac{F_P}{R} = \frac{F_p}{\sqrt{\left(r_{D(x)}\right)^2 + \left(r_{D(y)}\right)^2 + \left(r_{D(z)}\right)^2}} \quad (3)$$

The relative displacements $r_{D(x)}$, $r_{D(y)}$, $r_{D(z)}$ of the observed points are defined as [24-25]:

$$r_{D(x)} = D_{p(x)} - D_{d(x)}$$
$$r_{D(y)} = D_{p(y)} - D_{d(y)} \quad (4)$$
$$r_{D(z)} = D_{p(z)} - D_{d(z)}$$

where $r_{D(x)}$, $r_{D(y)}$, and $r_{D(z)}$ are the relative displacements for the points of bone segments (mm), $D_{p(x)}$, $D_{p(y)}$, and $D_{p(z)}$ are the displacements of the proximal bone segment (mm), and $D_{d(x)}$, $D_{d(y)}$, and $D_{d(z)}$ are the displacements of the distal bone segment in x, y, and z directions (mm).

IV. RESULTS

Figure 5 shows the displacement vectors due to the maximum axial load, where the course, direction, and intensity of the vectors for the analyzed points can easily be noticed. Table III shows the components of the displacement vectors and the displacement values for the maximum axial load of 200 N. The stiffness of the construction is determined using (2), based on the axial displacement in the z-axis direction (straight surface at the top of the proximal bone), while the fracture stiffness requires displacements at the proximal and distal bone segments at the fracture zone in the x, y, and z directions. This is done by observing which pair of points will result in the highest displacements, as shown in Figure 5 (detail A).

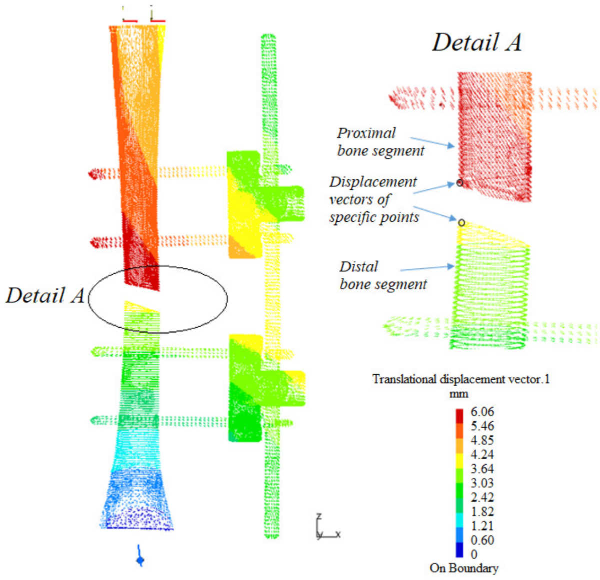

Fig. 5. Displacement vectors for the specific points under the impact of maximum axial load.

TABLE III. DISPLACEMENT AND STIFFNESS VALUES

Displacement of the proximal segment (mm)						Displacement of the distal segment (mm)			Fracture stiffness (N/mm)	Construction stiffness (N/mm)
Load zone			Fracture zone			Fracture zone				
x	y	z	$D_{p(x)}$	$D_{p(y)}$	$D_{p(z)}$	$D_{d(x)}$	$D_{d(y)}$	$D_{d(z)}$	C_{pp}	C_p
0	0	-4.54	3.593	0.616	-4.76	3.744	0.701	0.246	39.89	44.05

Figure 6 shows the von Mises distribution. Truss is an important component of the fixation device that needs to be considered in the structural analysis, which is loaded with eccentric pressure (simultaneous bending and pressure) for the truss amount σ_{vM}=318.62 MPa, which is also the global maximum.

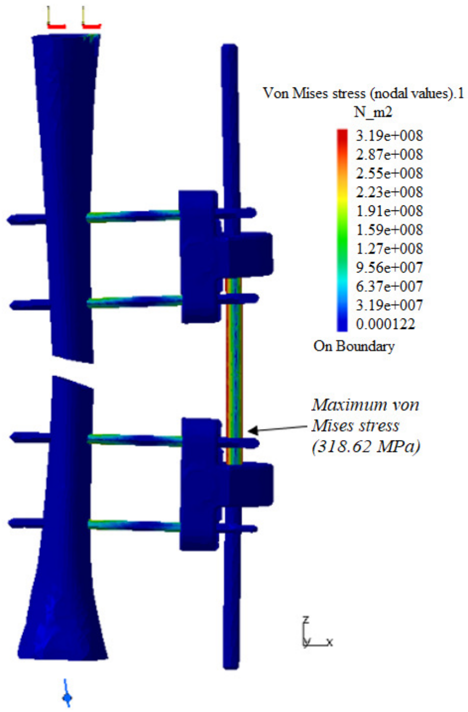

Fig. 6. Von Mises stress distribution.

Due to axial pressure, the bone is bent around the y-axis. This induces the location of the maximum stress at the bone circumference, i.e. the location of the peripheral points with the x-axis, as shown in Figure 7.

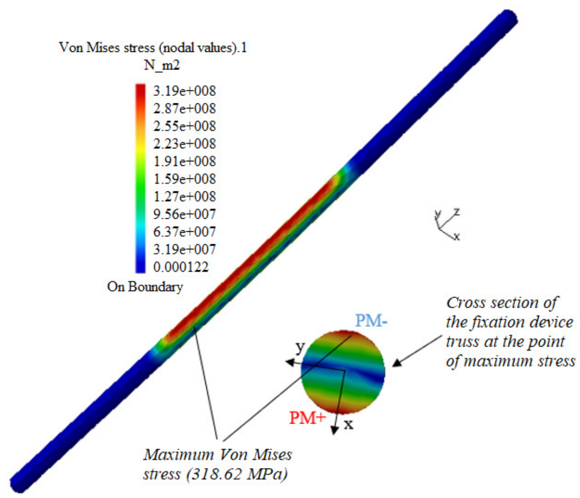

Fig. 7. Von Mises stress distribution for the fixation device truss.

The intensities and the direction of principal stresses were monitored for the 10 most critical zones of the device construction, as shown in Figure 8. Table IV summarizes the values of principal and von Mises stress for these points.

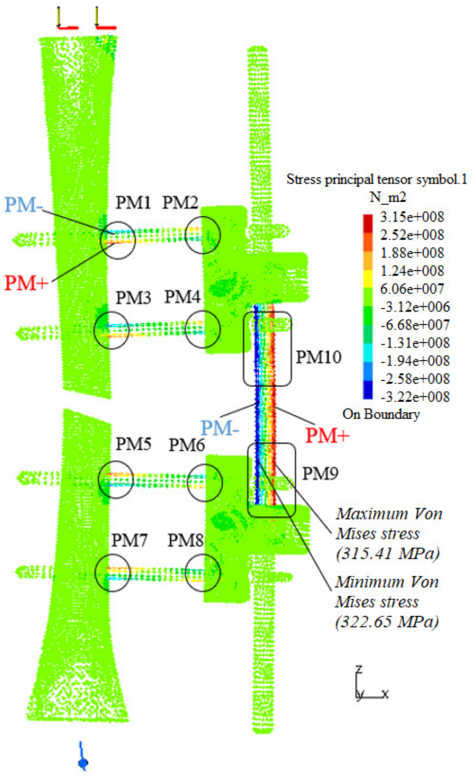

Fig. 8. Principal stresses at the critical zones of the construction.

TABLE IV. STRESS VALUES DUE TO AXIAL PRESSURE LOAD

Observed point	Principal stresses at critical points (MPa)						Von Mises stresses at critical points (MPa)	
	PM+			PM-			PM+	PM-
	σ_1	σ_2	σ_3	σ_1	σ_2	σ_3	σ_{vM}	σ_{vM}
1	198.0	-5.13	-14.4	-8.04	-11.2	-202	208.1	196.1
2	193.7	4.859	4.38	-3.35	-3.79	-175	191.1	174.8
3	203.4	11.83	7.18	-9.99	-14.2	-218	196.5	208.4
4	126.5	-6.46	-11.5	-3.22	-4.32	-185	135.6	183.7
5	205.6	10.64	7.23	-8.24	-13.8	-225	199.3	230.9
6	170.4	3.84	3.39	11.7	6.66	-145	169.2	145.5
7	218.8	13.95	9.70	-10.8	-12.3	-202	209.2	206.3
8	142.0	13.9	0.89	-3.02	-4.10	-163	147.2	162.5
9	315.4	1.07	2.20	0.42	-1.82	-322	318.8	317.3
10	302.9	1.41	0.51	6.36	5.89	-296	302.3	298.7

V. DISCUSSION

The maximum displacement in the device construction due to the impact of the axial load is located at the end of the second Schanz fastener and is 6.06 mm, as shown in Figure 5. Maximum displacements for the fracture zone are located at the edges of the proximal and distal bone segments, the values of which are given in Table III. When comparing these results with those of [26-27], it can be noticed that the Ultra X external fixation device has significantly higher displacements (80-100% higher) than the other such devices for the same case of applied load. Displacements in the load zone are used as a basis for the stiffness of the fixation device, which was 44.05 N/mm. If this value is compared with other studies [23-24], it can be observed that the stiffness of the Ultra X device is much lower (3-5 times) than that of other devices under the same load conditions. Similarly, displacements in the fracture zone are used to calculate the fracture stiffness, which is 39.89 N/mm and is again 3-5 times lower compared than the values found in [26-27]. The results of the structural analysis show that the most critical zone of the fixation device construction is the middle of the truss where it establishes contact with large spheres. This zone is a load transfer zone, where the axial force is transmitted from the couplings to the truss through the Schanz fasteners. The highest principal stresses, regarding the whole construction, were σ_1=315.41 MPa (global maximum) for the positive values and σ_3=-322.65 MPa (global minimum) for the negative values. Both extreme values are located in the truss, have similar values, and are in correspondence with the results obtained in other studies [26-27]. It is also important to note that stresses in the fixation device construction satisfy the maximum permissible stress of the device material.

VI. CONCLUSION

This study conducted a stability analysis on the Ultra X external fixation device due to the impact of axial loads, developing a FEM model. This model was used to observe the movements and displacements of the fracture and establish a connection between these phenomena with the stiffnesses of the fracture zone and the device itself. The analysis of the results obtained showed relatively large displacements compared to other studies for the same load conditions. This can be justified by the fact that a truss diameter of an Ultra X device has a smaller cross-section, i.e. moment of inertia. Lower displacement values could be expected for the hollow circle cross-sections of greater diameter, i.e. with an increased moment of inertia by moving away the material from the own axis of the element. This led to the conclusion that the mechanical stability of the Ultra X fixation device is insufficient for application to fractures of the lower extremities. However, the Ultra X device is recommended for traumas of the upper extremities due to its good properties, such as ease of implementation and small dimensions. In this case, weaker mechanical properties will not be a problem, as the upper extremities are subjected to significantly smaller loads.

REFERENCES

[1] T. N. Gardner, M. Evans, and J. Kenwright, "A biomechanical study on five unilateral external fracture fixation devices," *Clinical Biomechanics*, vol. 12, no. 2, pp. 87–96, Mar. 1997, https://doi.org/10.1016/S0268-0033(96)00051-4.

[2] C. S. Roberts, J. C. Dodds, K. Perry, D. Beck, D. Seligson, and M. J. Voor, "Hybrid External Fixation of the Proximal Tibia: Strategies to Improve Frame Stability," *Journal of Orthopaedic Trauma*, vol. 17, no. 6, Jul. 2003, Art. no. 415.

[3] C. Lenarz, G. Bledsoe, and J. T. Watson, "Circular External Fixation Frames with Divergent Half Pins: A Pilot Biomechanical Study," *Clinical Orthopaedics and Related Research*, vol. 466, no. 12, pp. 2933–2939, Dec. 2008, https://doi.org/10.1007/s11999-008-0492-0.

[4] R. G. Checketts and C. F. Young, "(iii) External fixation of diaphyseal fractures of the tibia," *Current Orthopaedics*, vol. 17, no. 3, pp. 176–189, Jun. 2003, https://doi.org/10.1016/S0268-0890(03)00068-9.

[5] A. Hutchinson, A. Frampton, and R. Bhattacharya, "Operative fixation for complex tibial fractures," *The Annals of The Royal College of Surgeons of England*, vol. 94, no. 1, pp. 34–38, Mar. 2012, https://doi.org/10.1308/003588412X13171221498668.

[6] L. Yang, M. Saleh, and S. Nayagam, "The effects of different wire and screw combinations on the stiffness of a hybrid external fixator," *Proceedings of the Institution of Mechanical Engineers, Part H: Journal of Engineering in Medicine*, vol. 214, no. 6, pp. 669–676, Jun. 2000, https://doi.org/10.1243/0954411001535697.

[7] J. Vossoughi, Y. Youm, M. Bosse, A. R. Burgess, and A. Poka, "Structural stiffness of the hoffmann simple anterior tibial external fixation frame," *Annals of biomedical engineering*, vol. 17, no. 2, pp. 127–141, Mar. 1989, https://doi.org/10.1007/BF02368023.

[8] T. K. Moroz, J. B. Finlay, C. H. Rorabeck, and R. B. Bourne, "Stability of the original Hoffmann and AO tubular external fixation devices," *Medical and Biological Engineering and Computing*, vol. 26, no. 3, pp. 271–276, May 1988, https://doi.org/10.1007/BF02447080.

[9] A. R. Remiger, "5. Mechanical properties of the Pinless external fixator on human tibiae," *Injury*, vol. 23, pp. S28–S43, Jan. 1992, https://doi.org/10.1016/0020-1383(92)90005-D.

[10] B. Fleming, D. Paley, T. Kristiansen, and M. Pope, "A Biomechanical Analysis of the Ilizarov External Fixator.," *Clinical Orthopaedics and Related Research (1976-2007)*, vol. 241, pp. 1976-2007, Apr. 1989.

[11] S. F. Fakhouri, M. M. Shimano, C. A. Araujo, H. L. Defino, and A. C. Shimano, "Photoelastic Analysis of the Vertebral Fixation System Using Different Screws," *Engineering, Technology & Applied Science Research*, vol. 2, no. 2, pp. 190–195, Apr. 2012, https://doi.org/10.48084/etasr.144.

[12] D. Benarbia, M. Benguediab, and S. Benguediab, "Two-dimensional Analysis of Cracks Propagation in Structures of Concrete," *Engineering, Technology & Applied Science Research*, vol. 3, no. 3, pp. 429–432, Jun. 2013, https://doi.org/10.48084/etasr.300.

[13] B. Achour, D. Ouinas, M. Touahmia, and M. Boukendakdji, "Buckling of Hybrid Composite Carbon/Epoxy/Aluminum Plates with Cutouts," *Engineering, Technology & Applied Science Research*, vol. 8, no. 1, pp. 2393–2398, Feb. 2018, https://doi.org/10.48084/etasr.1224.

[14] M. J. Bosse, C. Holmes, J. Vossoughi, and D. Alter, "Comparison of the Howmedica and Synthes Military External Fixation Frames," *Journal of Orthopaedic Trauma*, vol. 8, no. 2, pp. 119-126, Apr. 1994.

[15] R. N. Dehankar and A. M. Langde, "Finite Element Approach Used on the Human Tibia: A Study on Spiral Fractures," *Journal of Long-Term Effects of Medical Implants*, vol. 19, no. 4, pp. 313–321, 2009, https://doi.org/10.1615/JLongTermEffMedImplants.v19.i4.80.

[16] N. Pervan, A. J. Muminović, E. Mešić, M. Delić, and E. Muratović, "Analysis of Mechanical Stability for External Fixation Device in the Case of Anterior-Posterior Bending," *Advances in Science and Technology. Research Journal*, vol. 16, no. 3, pp. 136–142, Jul. 2022, https://doi.org/10.12913/22998624/146857.

[17] A. A. Shetty, U. Hansen, K. D. James, and S. Djozic, "Biomechanical Test Results of the Sarafix - External Fixator," Imperial College, London, UK, 2004.

[18] E. Mesic, N. Pervan, N. Repcic, and A. Muminovic, "Research of influential constructional parameters on the stability of the fixator Sarafix," in *Annals of DAAAM for 2012 & Proceedings of the 23rd International DAAAM Symposium*, Vienna, Austria, 2012.

[19] N. Pervan and E. Meši, "Stress Analysis of External Fixator Based on Stainless Steel and Composite Material," *International Journal of Mechanical Engineering and Technology*, vol. 8, no. 1, pp. 189–199, Jan. 2017.

[20] E. Mešić, N. Pervan, A. J. Muminović, A. Muminović, and M. Čolić, "Development of Knowledge-Based Engineering System for Structural Size Optimization of External Fixation Device," *Applied Sciences*, vol. 11, no. 22, Art. no. 10775, Jan. 2021, https://doi.org/10.3390/app112210775.

[21] E. Mešić, A. Muminović, M. Čolić, M. Petrović, and N. Pervan, "Development and Experimental Verification of a Generative CAD/FEM Model of an External Fixation Device," *Tehnički glasnik*, vol. 14, no. 1, pp. 1–6, Mar. 2020, https://doi.org/10.31803/tg-20191112161707.

[22] N. Pervan, E. Mešić, A. Muminović, M. Čolić, and M. Petrović, "Structural Size Optimization of an External Fixation Device," *Advances in Science and Technology. Research Journal*, vol. 14, no. 2, pp. 233–240, Jun. 2020, https://doi.org/10.12913/22998624/116870.

[23] M. Elmedin, A. Vahid, P. Nedim, and R. Nedžad, "Finite Element Analysis and Experimental Testing of Stiffness of the Sarafix External Fixator," *Procedia Engineering*, vol. 100, pp. 1598–1607, Jan. 2015, https://doi.org/10.1016/j.proeng.2015.01.533.

[24] E. Mešić, V. A. Avdić, and N. Pervan, "Numerical and experimental stress analysis of an external," *Folia Medica Facultatis Medicinae Universitatis Saraeviensis*, vol. 50, no. 1, 2015.

[25] Elmedin Mešić, Vahid Avdić, Nedim Pervan, and Adil Muminović, "A new Proposal on Analysis of the Interfragmentary Displacements in the Fracture Gap," *TEM Journal*, vol. 4, no. 3, pp. 270–275, 2015.

[26] N. Pervan *et al.*, "Biomechanical Performance Analysis of the Monolateral External Fixation Devices with Steel and Composite Material Frames under the Impact of Axial Load," *Applied Sciences*, vol. 12, no. 2, Jan. 2022, Art. no. 722, https://doi.org/10.3390/app12020722.

[27] N. Pervan, E. Mešić, A. J. Muminović, M. Delić, and E. Muratović, "Stiffness Analysis of the External Fixation System at Axial Pressure Load," *Advances in Science and Technology. Research Journal*, vol. 16, no. 3, pp. 226–233, Jul. 2022, https://doi.org/10.12913/22998624/149599.